BOLLETTINO DI GEOFISICA TEORICA ED APPLICATA VOL. 41, N. 1, pp. 1-20; MARCH 2000

Application of artificial neural networks for gravity interpretation in two dimensions: a test study

A. A. GRÊT [1], E. E. KLINGELÉ [2] and H.-G. KAHLE [2]

[1] *Department of Geophysics, Colorado School of Mines, Golden, USA*
[2] *Geodesy and Geodynamics Laboratory, ETH-Hönggerberg, Zürich Switzerland*

(Received August 24, 1999; accepted February 14, 2000)

Abstract. In applied geophysics generalized bodies are often used to model the distribution of underground masses, such as spheres, vertical cylinders, vertical prisms, etc. Generally, discrimination between disturbing bodies producing similar kinds of anomalies is extremely difficult, or even impossible, with classical algorithms. In this paper we present a technique for gravity interpretation, based on the application of feed-forward, multi-layer artificial neural networks (ANNs), trained with back-propagation algorithms. This technique is used, firstly, to discriminate bodies producing a similar kind of anomaly. When the general shape of the body has been found (qualitative interpretation), the ANN method is applied to find the shape parameters like depth, vertical extension and radius. It is shown that after having been properly trained, an ANN is able to recognize a disturbing body with a degree of confidence higher than 99%. It is also shown that inversions carried out with this method produce quantitative results with accuracy ranging from 2% to 5%. The applications presented in this paper are based on synthetic data. These are the first steps towards a generalized technique of interpretation.

1. Introduction

The aim of gravity interpretation is to discover how masses producing a given gravity anomaly are distributed. Although great efforts have been devoted to this topic, it has to be remarked that neither theoretical nor practical solutions to solve the problem completely exist. In applied geophysics, simple geometrical shapes are considered accurate enough for representing bodies. The most frequently used elementary shapes are spheres, cylinders, prisms and steps representing highly compact ore deposits, diamond-bearing pipes, dykes and vertical faults. At every stage of interpretation, the interpreter has to make choices between various possibilities that

Corresponding author: E. E. Klingelé; Institut für Geodäsie und Photogrammetrie; ETH-Hönggerberg, CH-8093 Zürich, phone: +41 1 633 2628; fax: +41 1 633 1066; e-mail: klingele@geod.baug.ethz.ch

are often biased. It is, for example, much easier to "see" structures on an anomaly map clearly, which support the preconceptions of a geologist or geophysicist, rather than to identify structures in an unknown area.

The goal of this study is to show how it is possible to avoid the effects of individual judgment by applying artificial neural networks (ANNs), to first discriminate disturbing bodies giving similar anomalies, and then use the same technique for inversion.

ANNs are biologically inspired; they are composed of elements behaving in a manner analogous to the most elementary functions of the biological neuron (McCulloch and Pitts, 1943). These elements are organized in a way that may be related to the anatomy of the brain. ANNs exhibit a surprising number of characteristics of the human brain. For example, they learn from experience, generalize from previous examples to new ones, and extract essential characteristics from inputs containing irrelevant data. ANNs can modify their behaviour in response to their environment. This factor, more than any other, is responsible for the interest they have received. If ANNs receive a set of inputs (perhaps with desired outputs), they self-adjust to produce consistent responses. Once trained, a network's response can be, to a certain degree, insensitive to slight variations in its input. Most ANNs contain only the simplest characteristics of the human brain. The artificial neuron was designed to mimic the first-order characteristics of the biological neuron. In essence, a set of inputs is applied, each representing the output of another neuron. Each input is multiplied by a corresponding weight, analogous to a synaptic strength, and all of the weighted inputs are then summed to determine the activation level of the neuron. The net signal is usually further processed by an activation function to produce the neuron's output signal (Grossberg, 1973). This may be a simple linear function, it may also be a threshold function (called a squashing function) that simulates more accurately the non-linear transfer characteristic of the biological neuron and permits more general network functions. Although a single neuron can perform certain simple-pattern detection functions, the power of neural computation comes from connecting neurons to networks. The simplest network is a layer. Each element of the set of inputs is connected to an artificial neuron through a separate weight. What each neuron outputs is simply a weighted sum of the inputs to the network. Multi-layer networks have been proven to have capabilities beyond those of a single layer, and in recent years, algorithms have been developed to train them. Multi-layer networks may be formed by simple cascading groups of single layers: the output of one layer provides the input for the subsequent layer. The first layer receives the input signal whereas the last one gives the output signal. The layers between the input and the output ones are called hidden layers. These networks have no feedback connections, that is, connections through weights extending from the outputs of a layer to the inputs of the same layer or previous layers. This special class called non-recurrent or feed-forward networks, is of considerable interest, and is widely applied.

To be useful an artificial network has to be trained in such a way that the application of a set of inputs produces the desired (or at least consistent) set of outputs. Training is accomplished by sequentially applying input vectors, and network weights are adjusted according to a predetermined procedure. During training, the network weights gradually converge to such values that each input vector produces the desired output vector. Usually, a network is trained

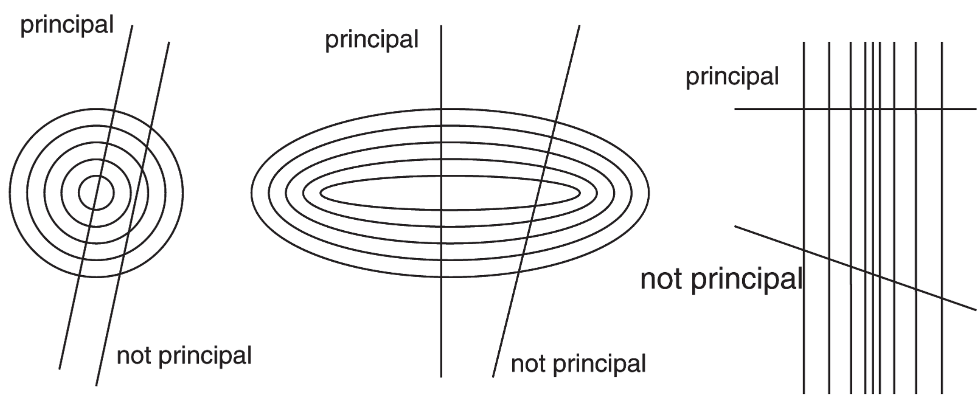

Fig. 1 - Definition of ***principal*** and ***not principal*** profiles for different kinds of gravity anomalies.

over a number of such training pairs. When an input vector is applied, the output of the network is calculated and compared to the corresponding target vector, and the difference (error) is fed back through the network, and weights are changed according to an algorithm that tends to minimize the error. The vectors of the training set are applied sequentially, errors are calculated, and weights are changed according to an algorithm that tends to minimize the error.

Large and complex networks generally offer great computational capabilities; they are built in configurations inspired by the layered structure of certain portions of the brain.

To be useful, an artificial network first must be trained with a set of data covering the complete range of values possible for a given case. More detailed explanations about the structure, training theory and algorithms of ANN can be found in many textbooks. See for example: Wasserma (1989), Freeman and Skapura (1991), Hertz et al. (1991), Rumelhart and Lelland (1989), Hecht-Nielsen (1990), Simpson(1990). In this article only feed-forward ANN and back-propagation training-algorithms are used.

2. Concept of the gravity interpretation with ANN

For the interpretation in two dimensions a residual anomaly, along a principal profile, must be available. A principal profile is defined as a profile passing through the maximum of the anomaly and crossing the anomaly lines perpendicularly, see Fig. 1. From the shape of the anomaly and/or geological information the interpreter has to choose the category of the disturbing bodies. It is clear that there is usually no ambiguity between the anomaly produced by a sphere and the one produced by a dyke. However, as in all geophysical data-interpretations one needs to have some idea about the target. With the geological information available, the minimal and maximal possible values of the disturbing body's shape can be determined. In other words, it makes no sense to train an ANN for a depth of hundreds of meters when the target produces an anomaly of a few microgals, with a wavelength of some meters. If only poor information on the target exists, the training space chosen can be very large, but this will increase training time and will require more effort to find a satisfying result. In order to train an ANN for body-recognition, it is necessary to calculate anomalies for bodies belonging to the same category (e.g. sphere and vertical cylinder, dyke and horizontal cylinder; anticline and syncline) and with parameters falling within the boundaries given by geological information. No assumptions on the density contrast are needed for body recognition.

After the ANN has chosen among the competing bodies, quantitative interpretation can begin.

3. Application for qualitative interpretation

3.1. Introduction

Bodies producing circular and almost concentric contours on the anomaly map are supposed to be spheres, circular discs or vertical cylinders. The presence of thin dykes, veins and mineralized shear zones are shown by elliptic contours, the major axis defining the strike direction. If the contour map exhibits symmetry around the maximum anomaly line, the models that could be assumed are vertical dykes, anticlines and synclines, depending on the local geology. Gravity anomalies caused by structures of simple geometry are characterized by various parameters that completely define their density contrast and their orientation below the ground surface. The magnitude of the anomaly is mostly a measure of the density contrast, whereas its shape includes all other parameters of the model, often known as shape parameters. However, it is not a simple task to choose between two or more bodies producing similar anomalies. Apart from the fact that the classical procedures used for this task are tedious, they are also subject to mistakes due to the importance of the subjective judgement. Because of **ANN's** (Artificial Neural Network) capability to classify things into groups, this leads to the idea that an ANN can be trained with a set of computed anomalies to recognize different bodies, and then used to recognize the model for other anomalies. A second well-known application of ANN is to learn from examples and then conclude for similarity. This means that an ANN can be trained with a set of synthetic anomalies and their corresponding target parameters, and can then find the corresponding model parameters from an experimental anomaly (not included in this training set). Looking at a gravity map it is easy to distinguish between Central Symmetric and Axial Symmetric anomalies (Fig. 2). The problem arises, when one tries to find the shape of the disturbing body producing one of these anomalies.

A circular anomaly can be produced either by a sphere or by a vertical cylinder, whereas an elliptical anomaly (2D) can be caused either by a horizontal cylinder or by a vertical dyke (Fig. 2). Only a very experienced interpreter, if at all, is able to recognize the shape of a disturbing body from the shape of an anomaly. If an ANN is trained with a set of anomalies produced by spheres and by vertical cylinders, it is able to decide which kind of body is producing the anomaly.

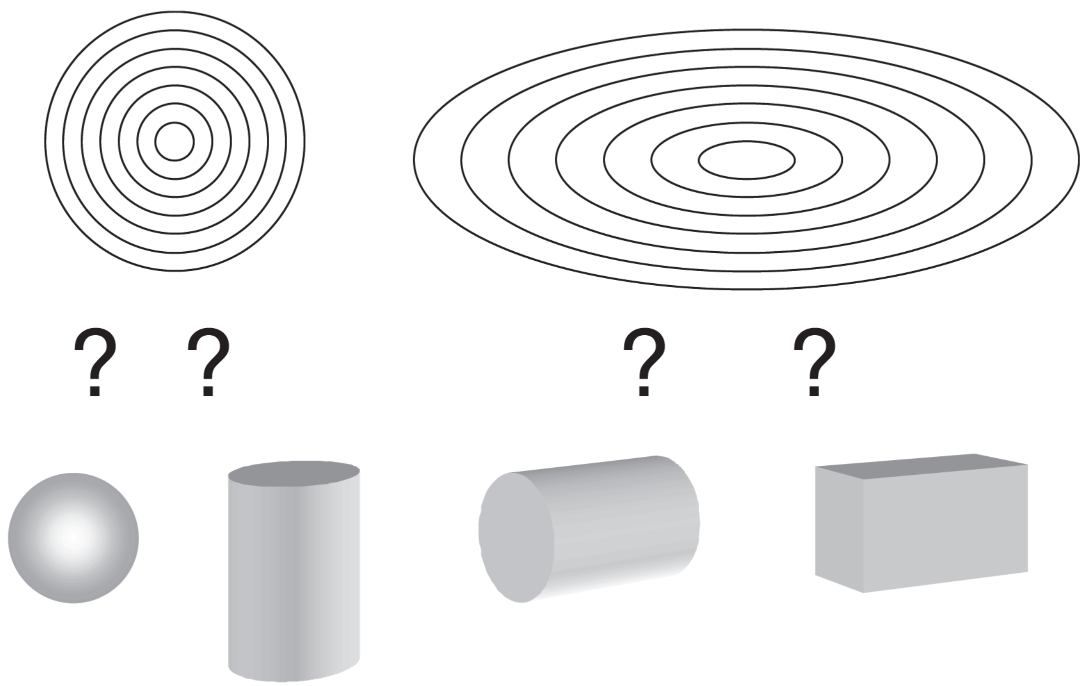

Fig. 2 - Schematic description of the ambiguity in gravity anomaly interpretation.

3.2. Criteria for anomaly recognition

Different features that define the shape of a disturbing body can be derived from an anomaly along a principle profile (tangent, location of inflection point, maximal value,…). The shape of the anomaly depends only on the shape of the body and not on its dimensions. Therefore, the absolute values of the anomaly are not necessary.

In order to recognize a sphere or a vertical cylinder, only two features are necessary, whereas for a horizontal cylinder or a vertical dyke three features are needed. The different features used to characterize the anomalies are defined in Fig. 3.

It is worth noting that there is no general rule for finding the number of necessary features. An ANN trained with four features may work as well as, or even better, than one trained with three, but the training-time will certainly increase.

3.3. Examples

For training-sets and application-sets, spheres, horizontal cylinders and vertical dykes were computed by means of their analytic formulas. The shape parameters of these bodies are summarized in Fig. 4.

Each training-set contains input vectors and the corresponding target vectors. The previously

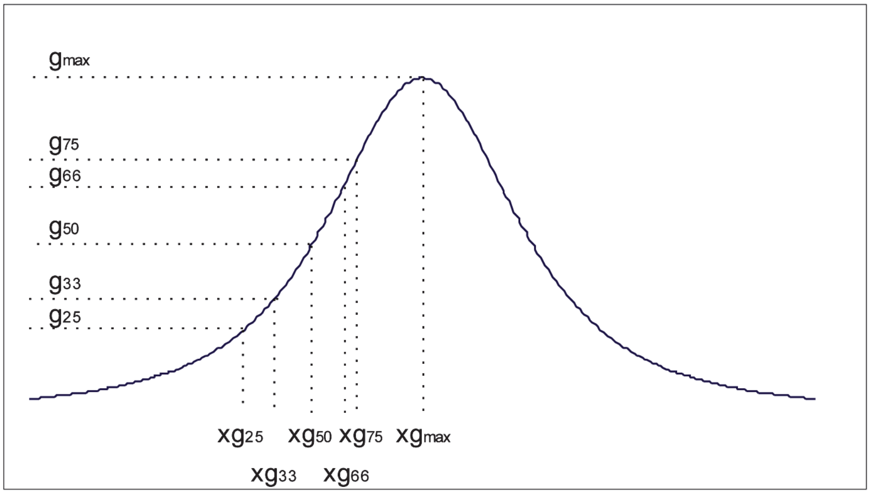

$$F1 = \frac{xg_{50}}{xg_{75}} \qquad F2 = \frac{(xg_{25} - xg_{66})}{(xg_{66} - xg_{75})}$$

$$F3 = \frac{xg_{75}}{xg_{50}} \qquad F4 = \frac{(xg_{50} - xg_{75})}{(xg_{25} - xg_{50})}$$

$$F5 = \frac{xg_{25}}{xg_{50}}$$

where: $F1$ to $F5$ are the features for the description of the anomalies
g_y is the value of g at $y\%$ of g_{max}
xg_y is the value of x at g_y.

Fig. 3 - Definition of the features describing the shape of the anomalies.

defined features form the input vectors. The target vectors contain the expected results. The target vector (1, 0) for example, represents spheres, and the vector (0, 1) represents vertical cylinders. Fig. 5 shows this relationship for spheres and vertical cylinders as well as for horizontal cylinders, vertical dykes, anticlines and synclines, respectively. Each application-set, contrary to the training-set, contains only the input vectors.

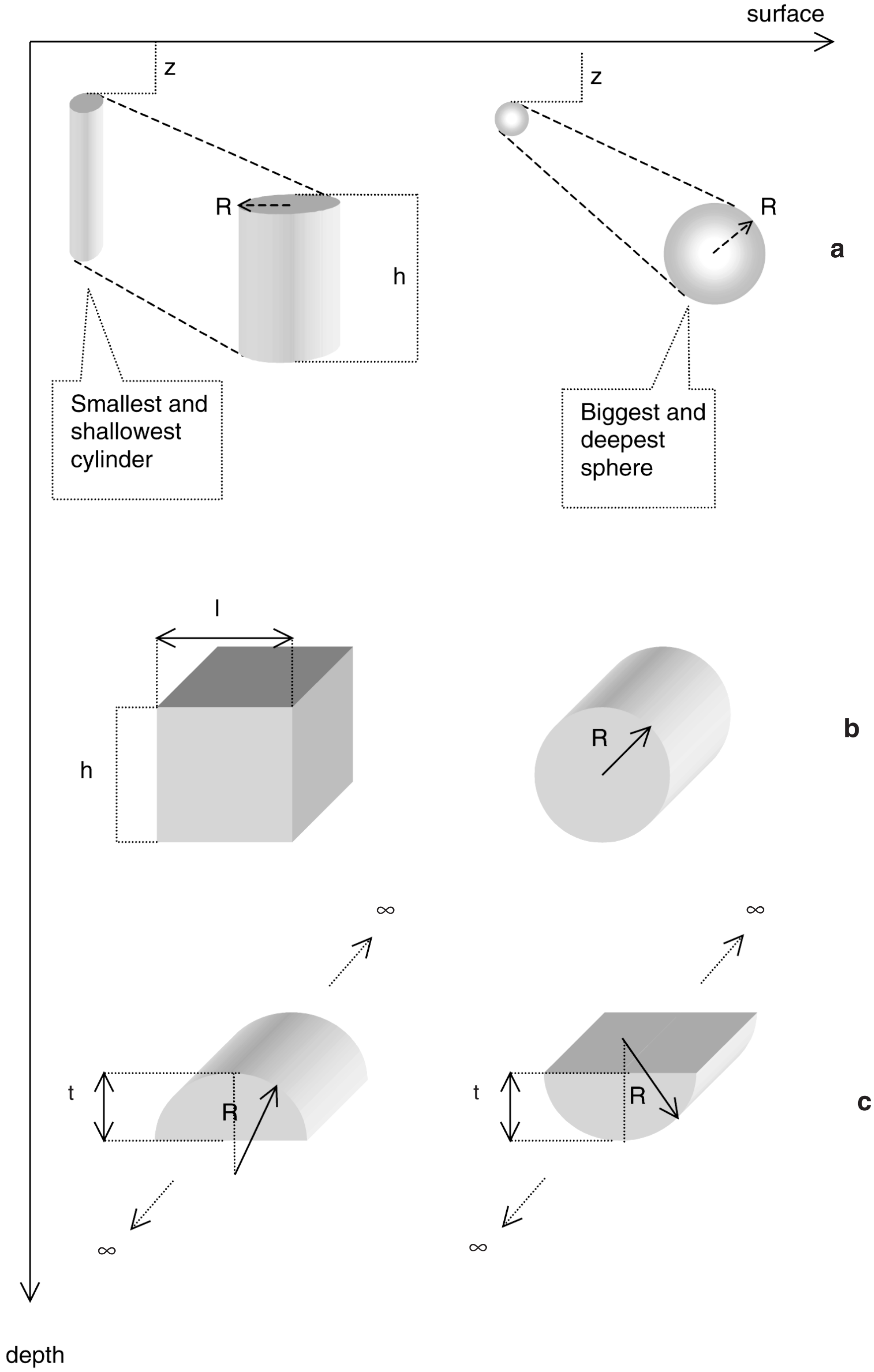

Fig. 4 - Definition of the bodies and their parameters representing: (a) spheres and vertical cylinders; **Z** = depth of the top of the structure, **R** = radius, **h** = vertical extension, (b) horizontal prisms and horizontal cylinders (principle profile); and **l** = width of the prism, (c) anticlines and synclines and their appearance on the anomaly map; **t** = thickness. Note that the body gets larger when **R** increases and not when t is changed.

Table 1 - Values of the application-set and the corresponding results.

body	z [m]	h [m]	R [m]	ρ [kg/m^3]	a_1 (sphere)	a_2 (cylinder)
S	350	----	150	1000	1.0000	0.0000
C	350	1350	150	1000	0.0002	1.0000
S	425	----	225	1000	1.0000	0.0000
C	425	1450	225	1000	0.0004	0.9999
S	650	----	190	1000	1.0000	0.0000
C	650	1510	190	1000	0.0003	0.9999
S	685	----	240	1000	1.0000	0.0000
C	685	1625	240	1000	0.0002	1.0000
S	700	----	110	1000	1.0000	0.0000
C	700	1725	110	1000	0.0002	1.0000
S	725	----	210	1000	1.0000	0.0000
C	725	1680	210	1000	0.0002	1.0000

C = vertical cylinder; **S** = sphere; **z** = depth; **h** = vertical extension of cylinder; **R** = radius; all these units are in [m]; ρ= density contrast [kg/m^3]; $\mathbf{a_1}$ = answer of the ANN corresponding to the **S**phere; $\mathbf{a_2}$ = answer of the ANN corresponding to the **C**ylinder.

3.4. Training

SPHERES AN VERTICAL CYLINDERS. - An ANN with 2 neurons in its hidden layer (2,2,2) was trained for the spheres and the vertical cylinders. The tops of the cylinders were set between 250 m and 750 m below the surface and their radii between 100 m and 250 m, with 250 m and 150 m increments for depths and radii, respectively. Their vertical extension is 1000 m and the density contrast was set to one. Gravity anomalies for spheres were calculated for the same depth of the top and the same radii as the cylinders, the density contrast was also set to one.

HORIZONTAL CYLINDER AND VERTICAL PRISM. - Horizontal cylinders and vertical prisms are often used in micro-gravimetry, because they represent good models for tunnels. The tops of the structures were set between 2 m and 4 m, the radius of the cylinder between 1 m and 2 m, the width of the prism between 2 m and 4 m and its vertical extension between 1 m and 7 m. All the increments were 0.25 m.

Because the difference between the shape of the anomalies is much smaller than for a sphere and vertical cylinder the training vectors have to contain three features instead of two (F3, F4 and F5).

ANTICLINES AND SYNCLINES. - The geometry of bodies representing synclines or anticlines is not so obvious as the above examples; there are different ways to approximate these shapes. The simple bodies used to represent an anticline and a syncline are defined in Fig. 4c. An (3,3,2) ANN was trained with a set containing the features F3, F4 and F5 calculated for 20 anticlines and 20 synclines with the same dimensions. These dimensions were: Zmin=200 m, Zmax=800 m, Rmin=1000 m, Rmax=1500 m, tmin=200 m, tmax=800 m. The increments were 3 m for *Z* and t, and 1 m for *R*.

Table 2 - Values of the second test-set and the corresponding results.

body	z [m]	h [m]	R [m]	ρ [kg/m^3]	a_1 (sphere)	a_2 (cylinder)
S	350	----	150	500	1.0000	0.0000
C	350	1350	150	500	0.0002	1.0000
S	425	----	225	500	1.0000	0.0000
C	425	1450	225	500	0.0004	0.9999
S	650	----	190	500	1.0000	0.0000
C	650	1510	190	500	0.0003	0.9999
S	685	----	240	500	1.0000	0.0000
C	685	1625	240	500	0.0002	1.0000
S	700	----	110	500	1.0000	0.0000
C	700	1725	110	500	0.0002	1.0000
S	725	----	210	500	1.0000	0.0000
C	725	1680	210	500	0.0002	1.0000

C = vertical cylinder; **S** = sphere; **z** = depth; **h** = vertical extension of cylinder; **R** = radius; all these units are in [m]; ρ= density contrast [kg/m^3]; $\mathbf{a_1}$ = answer of the ANN corresponding to the **S**phere; $\mathbf{a_2}$ = answer of the ANN corresponding to **C**ylinder.

3.5. Results

SPHERE AND VERTICAL CYLINDER. - A test-set, with the parameters listed in Table 1 was passed through the trained ANN. The output ($\mathbf{a}_1$, $\mathbf{a}_2$) is presented on the right of the same table.

When the output (from the corresponding neuron) is near 1 it is very probable that the ANN recognized the right body. However, it is always necessary to look at both outputs. When the sum of $\mathbf{a}_1$ and $\mathbf{a}_2$ is not close to 1, the result cannot be trusted at all. With this thought in mind, the above results are with a very high probability correct.

In order to demonstrate the ability of the ANN to recognize the true body, independently of the density, a second application-set for the same parameters as in Table 4 but with a density contrast of 500 [kg/m^3] instead of 1000 [kg/m^3] was calculated and then passed through the same network. As expected the result is exactly the same (see Table 2).

HORIZONTAL CYLINDER AND VERTICAL PRISM. - An application-set with twenty bodies was calculated and passed through the ANN. The dimensions and the network outputs are listed in Table 3. The network recognized all bodies correctly, however, the third body produced an output of (0.3689, 0.6373) and the sum of the two output-neurons is (1.0062). This shows that the body is recognized as a vertical prism, but only with a high degree of uncertainty.

This result is reasonable because the vertical extension of the prism is exactly the same as its width and is very close to a horizontal cylinder with the same dimensions. Therefore, the resemblance to a horizontal cylinder is evident.

ANTICLINE AND SYNCLINE. - To demonstrate the behaviour of an ANN trained with anticlines and synclines, a test-set containing six input vectors for both structures was computed. The

Table 3 - Values of the parameters of the application-set and the corresponding results.

Nr.	Body	z [m]	h [m]	2R [m] or l [m]	a_1 (cylinder)	a_2 (prism)
1	P	2.10	5.10	2.00	0.0000	1.0000
2	C	2.10	----	2.00	0.9999	0.0001
3	P	3.10	5.10	2.00	0.3689	0.6373
4	C	3.10	----	2.00	0.9999	0.0001
5	P	3.00	6.00	2.50	0.0001	0.9999
6	C	3.00	----	2.50	0.9965	0.0033
7	P	3.00	8.00	2.50	0.0000	1.0000
8	C	3.00	----	2.50	0.9953	0.0045
9	P	2.50	7.00	2.50	0.0000	1.0000
10	C	2.50	----	2.50	0.9999	0.0001
11	P	3.50	7.00	2.50	0.0000	1.0000
12	C	3.50	----	2.50	0.9998	0.0002
13	P	3.00	6.00	3.50	0.0000	1.0000
14	C	3.00	----	3.50	0.9965	0.0033
15	P	3.00	8.00	3.50	0.0000	1.0000
16	C	3.00	----	3.50	0.9955	0.0044
17	P	2.50	7.00	3.50	0.0000	1.0000
18	C	2.50	----	3.50	0.9999	0.0001
19	P	3.50	7.00	3.50	0.0000	1.0000
20	C	3.50	----	3.50	0.9998	0.0002

C = horizontal cylinder; **P** = vertical prim; **z** = depth; **h** = vertical extension of prism; **R** = radius of cylinder; **l** = width of prism; all the units are in [m]; $\mathbf{a_1}$ = answer of the ANN corresponding to the **S**phere; $\mathbf{a_2}$ = answer of the ANN corresponding to the **C**ylinder.

dimensions and the corresponding network outputs are listed in Table 4.

4. Application for quantitative interpretation

4.1. Introduction

In the inversion methods a general hypothesis on the model is made and initial values are attributed to the model-parameters. The method then optimizes these parameters directly in the sense that they are the best values obtainable for a given anomaly.

Doing inversion with ANNs, the above order is changed such that a network is trained for a wide range of model-parameters. Once trained, an ANN is able to find the best parameters for a given model without any optimization.

4.2. Criteria for inversion

Some of the features used to describe an anomaly were already explained in the previous

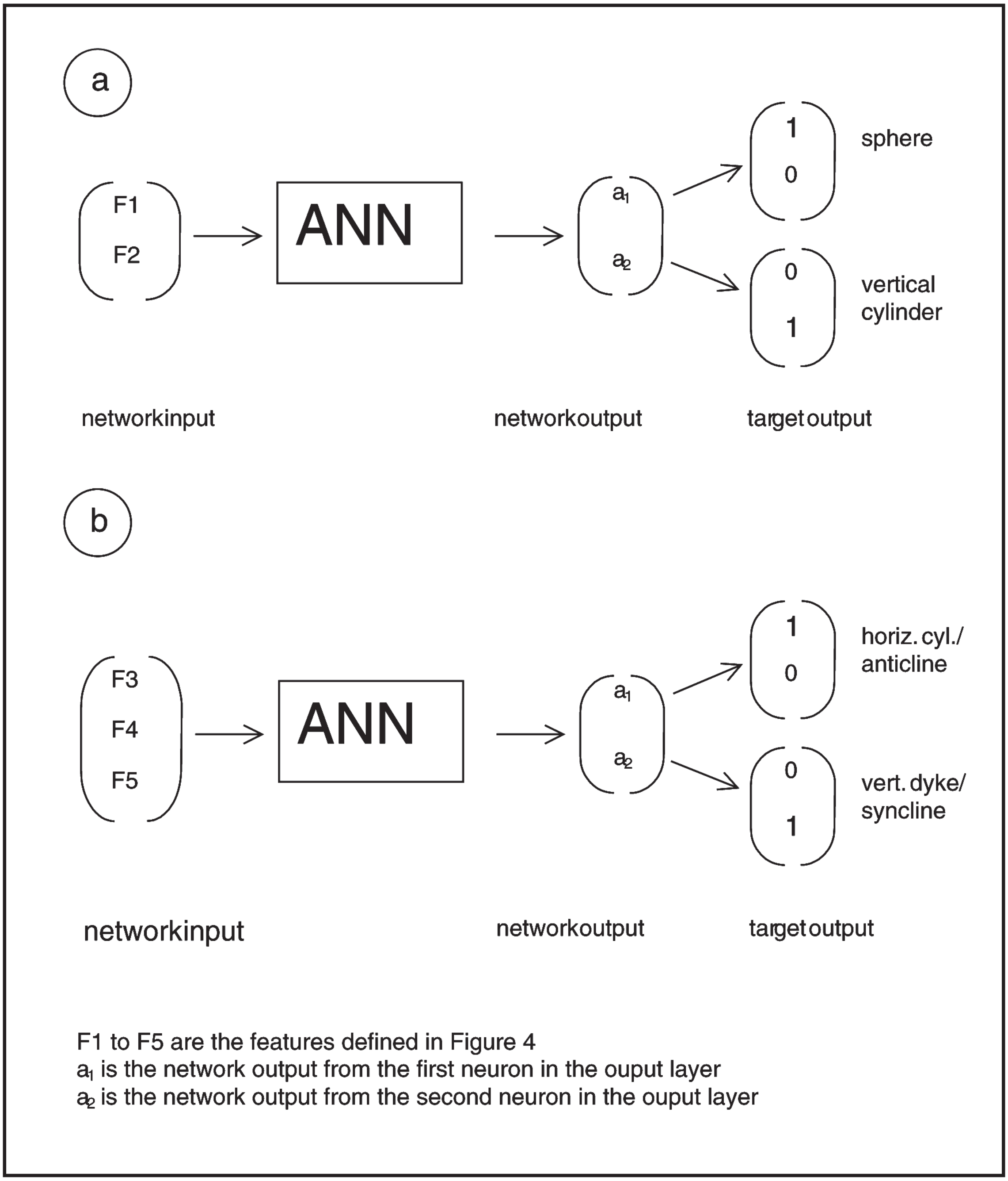

Fig. 5 - Schematic description of the input-output relationship of an ANN used to recognize the geometry of a disturbing body. a) For sphere and vertical cylinder and b) for horizontal cylinder, vertical dyke, anticline and syncline.

chapter. Inversion is a more sophisticated problem than the simple recognition of the shape of a body and demands a more precise description of the anomalies. Fig. 6 defines the additional features used for the inversion process.

Each body's anomaly is sensitive to different features and some bodies need more fea-

Table 4 - Values of the test-set and the corresponding results.

Nr.	body	z [m]	h [m]	R [m]	a_1 (anticline)	a_2 (syncline)
1	A	300	700	1250	1.0000	0.0000
2	S	300	700	1250	0.0000	1.0000
3	A	300	900	1250	1.0000	0.0000
4	S	300	900	1250	0.0000	1.0000
5	A	500	900	1250	1.0000	0.0000
6	S	500	900	1250	0.0000	1.0000
7	A	210	420	1010	1.0000	0.0000
8	S	210	420	1010	0.0000	1.0000
9	A	410	620	1010	1.0000	0.0000
10	S	410	620	1010	0.0000	1.0000
11	A	610	820	1010	1.0000	0.0000
12	S	610	820	1010	0.0000	1.0000

A = anticline; **S** = syncline; **z** = depth; **h** = vertical extension; **R** = radius; all units are in (m); $\mathbf{a_1}$ = network output for the first neuron in the output layer, corresponding to the answer for **A**; $\mathbf{a_1}$ = answer of the ANN corresponding to the **S**phere; $\mathbf{a_2}$ = answer of the ANN corresponding to the **C**ylinder.

tures than others. A list of the different bodies with their corresponding features is shown in Table 5.

4.3. Examples

Like for body-recognition, each training-set contains input vectors and corresponding target vectors. The previously defined features form the input vectors and the target vectors contain the expected results (model-parameters). Note that for each category of body, a different ANN is trained with a number of input-output-vector pairs that define the capacity of the ANN. Probably the most difficult task in quantitative gravity interpretation is to find the density for a disturbing body. No inversion technique is able to find all shape parameters and the density, without ambiguity. Once the shape of a disturbing body is known, the density can easily be calculated with the analytic formula or with numerical integration. However, when the shape parameters are wrong, the density will be wrong too. We attempted here to find as precise as possible shape parameters without including the effect of density. An assumption on the density is made and the ANN is trained for that density, the effect of a variation on density is tested after training. When a large change in density results in a small change in the shape of the body, the network can be used to find precise enough shape parameters, so that the right density can be calculated afterwards.

4.4. Training

The same kind of ANN used for model recognition is trained to solve the inversion problem.

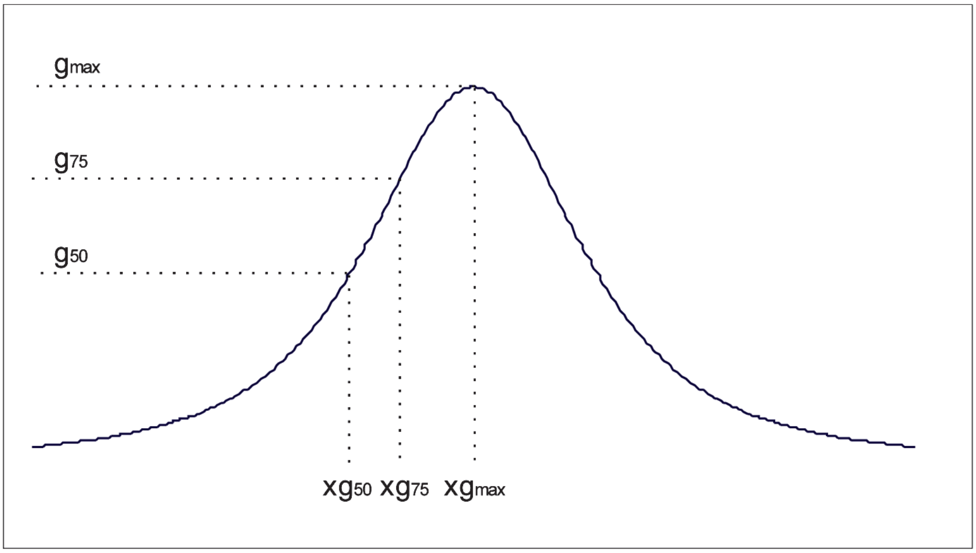

$$F6 = \int g(x)dx \qquad F7 = xg_{50}$$

$$F8 = xg_{75} \qquad F9 = g_{\max}$$

where: $F6$ to $F9$ are the additional features for the description of the anomalies
g_y is the value of g at $y\%$ of the maximal value
xg_y is the value of x at g_y.

Fig. 6 - Definition of the additional features F6, F7, F8 and F9 describing the shape of the anomalies.

Because the problem is much more complicated than the simple discrimination, the ANN is very sensitive to local minimum in the "multi-dimensional error surface". The larger a network is, the more variations on this surface exist. In consequence a very powerful network could find the target vectors in the training set very precisely and could yield poor results for parameters not corresponding to the training set. The number of neurons in the hidden layer is crucial for the problem but no rules exist for the determination of the optimal dimension of an ANN. Because the training process often falls in local minimum, a more powerful back-propagation algorithm than the simple steepest descent was used (Levenberg-Marquardt back-propagation approximation; Hagan and Menhaj, 1994).

Table 5 - List of the bodies with their corresponding features.

body	F1	F2	F3	F4	F5	F6	F7	F8	F9
sphere						P	P	P	
vertical prism			P	P		P			
horizontal cylinder						P	P	P	
vertical cylinder	P	P				P			P
anticline				P			P	P	P
syncline				P			P	P	P

SPHERES, HORIZONTAL CYLINDERS AND VERTICAL PRISMS. - An (3.2.2) ANN was trained for these structures with constant density contrasts of 300 kg/m^3 for the spheres and the vertical prisms, and of 2500 kg/m^3 for the horizontal cylinders. This latter density contrast was chosen because the model mostly represents tunnels or other kinds of cavities. The neurons of the input layers correspond to density, radius and depth of the center of mass for the spheres and the horizontal cylinders, and to density, top and thickness for the vertical dykes. The neurons of the output layers correspond to the same parameters except for the density.

The training parameters of these bodies are summarized in Table 6.

VERTICAL CYLINDERS, SYNCLINES AND ANTCLINES. - An (4.3.3) ANN was trained for these bodies with a density contrast of 300 kg/m^3. The neurons of the input layers correspond to density, radius, and depth of the top of the structure and vertical extension whereas the neurons of the output layers correspond to the same parameters with the exception of the density which is not resolved.

The training parameters of these bodies are summarized in Table 6.

4.5. Results

In order to test the capacity of the ANN objectively, all the geometrical parameters for each model were randomly generated but strictly maintained inside the training space. On the opposite side, the density contrasts were set between 290 and 300 kg/m^3 for the bodies trained with 300 kg/m^3 and between 2400 and 2600 kg/m^3 for the horizontal cylinder. These changes were made in order to find out if the technique permits some inaccuracies of the density contrasts without degrading the accuracy of the results. After passing the application-set through the network, the difference between the resulting output and the target parameters (network-error) was calculated for each body.

SPHERES. - An application-set containing 317 pairs of input- and target-vectors was used for the test. The standard deviations of the differences between the real and the computed depth and

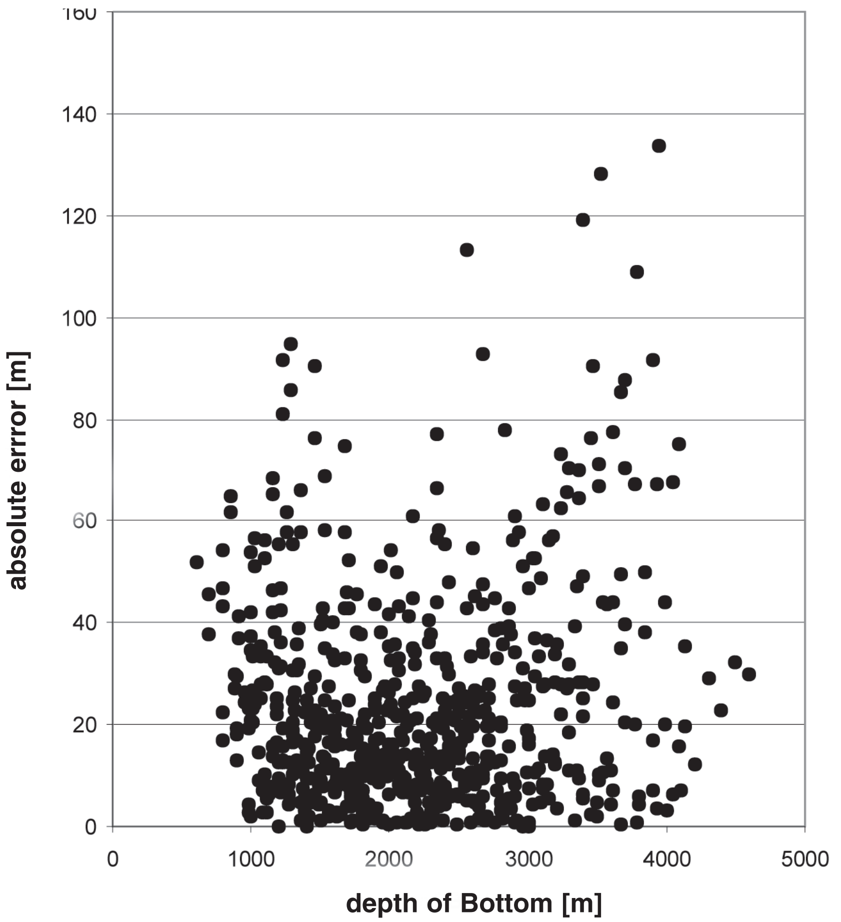

Fig. 7 - Values of the depth of the bottom of the vertical cylinders obtained by the inversion with an (3.2.2) ANN. The absolute error is shown as a function of the true depth.

radius are 5.5 m and 3.7 m respectively. Considering the large values chosen for these parameters the standard deviation values are surprisingly small. For the smallest sphere (198 m) this corresponds to an error of 2.8% and of 1.1% for the largest sphere (517 m). For the shallowest body (115 m) it corresponds to an error of 3.2% and for the deepest (245 m) to an error of 1.5%.

HORIZONTAL CYLINDERS. - For this test an application-set with 225 pairs of input- and target-vectors was used. The standard deviations of the differences between the real and the computed depth and radius are 0.02 m and 0.015 m respectively. For the smallest cylinder (1.01 m) this results in an error of 1.49% and for the largest cylinder (3.99 m) in an error of 0.38%. For the shallowest body (2.26 m) it corresponds to an error of 0.89% and for the deepest (8.53 m) to an error of 0.23%.

VERTICAL PRISMS. - The standard deviations of the differences between the real and the com-

Table 6 - Summary of the geometrical parameters used for training spheres, horizontal cylinders, vertical cylinders, vertical dykes, anticlines and synclines. The parameters are defined in Fig. 4. The units are in meters. The subscript inc. means increment.

Z_{ma}	Z_{mi}	Z_{inc}	R_{ma}	R_{mi}	R_{inc}	h_{ma}	h_{mi}	h_{inc}	l_{ma}	l_{mi}	l_{inc}	Body
150	550	50	100	250	50	-----	-----	-----	-----	-----	-----	Sphere
1	5	0.5	1	4	0.25	-----	-----	-----	-----	-----	-----	H. Cyl.
10	50	10	-----	-----	-----	400	400	0	10	60	10	V. Prism
200	600	100	200	1000	200	400	4000	400	-----	-----	-----	V. Cyl.
300	500	50	300	700	50	250	400	50	-----	-----	-----	Anticline
300	500	50	300	700	50	250	400	50	-----	-----	-----	Syncline

puted data for an application–set containing 209 pairs of vectors, is 0.2 m for the depth and 0.3 m for the width. For the shallowest body (11.13 m) it corresponds to an error of 1.8% and for the deepest (49.1 m) to an error of 0.41%. For the narrowest dyke (12.77 m) this corresponds to an error of 2.35% and for the widest (57.38 m) to an error of 0.52%.

VERTICAL CYLINDER. - A test-set with 637 pairs of input- and target-vectors was used in this case. The standard deviations of the differences between the real and the computed depth, vertical extension and radius are 8.8 m, 61.2 m respectively 14.8 m. For the shallowest body (200 m) it results in an error of 4.4% and for the deepest (600 m) in an error of 1.47%. For the cylinder with the smallest vertical extension (600 m) this corresponds to an error of 4.2% and for the largest (4600 m) to an error of 1.33%. For the cylinder with the smallest radius (200 m) it results in an error of 4.4% and for the largest (100 m) in one of 1.48%.

ANTICLINE. - An application-set with 409 pairs of input- and target-vectors was used. The standard deviations of the differences between the real and the computed top, bottom and radius are 3.3 m, 5.6 m and 8.8 m respectively. For the shallowest body (290.2 m) it corresponds to an error of 1.14% and for the deepest (509.7 m) to an error of 0.65%. For the anticline with the smallest vertical extension (bottom at 545.2 m) this results in an error of 1.03% and for the largest (900 m) in an error of 0.62%. For the anticline with the smallest radius (290.5 m) it results in an error of 3.03% and for the largest (727.7 m) in one of 1.21%.

SYNCLINES. - Exactly the same parameters as for the anticline were used for testing the syncline. The standard deviations of the differences between the real and the computed top, bottom and radius are 3.6 m, 5.3 m and 10.2 m respectively. For the shallowest body (290.2 m) it corresponds to an error of 1.24% and for the deepest (509.7 m) to an error of 0.71%. For the anticline with the smallest vertical extension (bottom at 545.2 m) this results in an error of 0.97% and for the largest (900 m) in an error of 0.59%. For the anticline with the smallest radius (290.5 m) it results in an error of 3.51% and for the largest (727.7 m) in one of 1.4%.

In order to better illustrate these results, the values obtained for the depth of the bottom of the vertical cylinder are shown in Fig. 7. Figs. 8 and 9 show the values obtained for the radius of

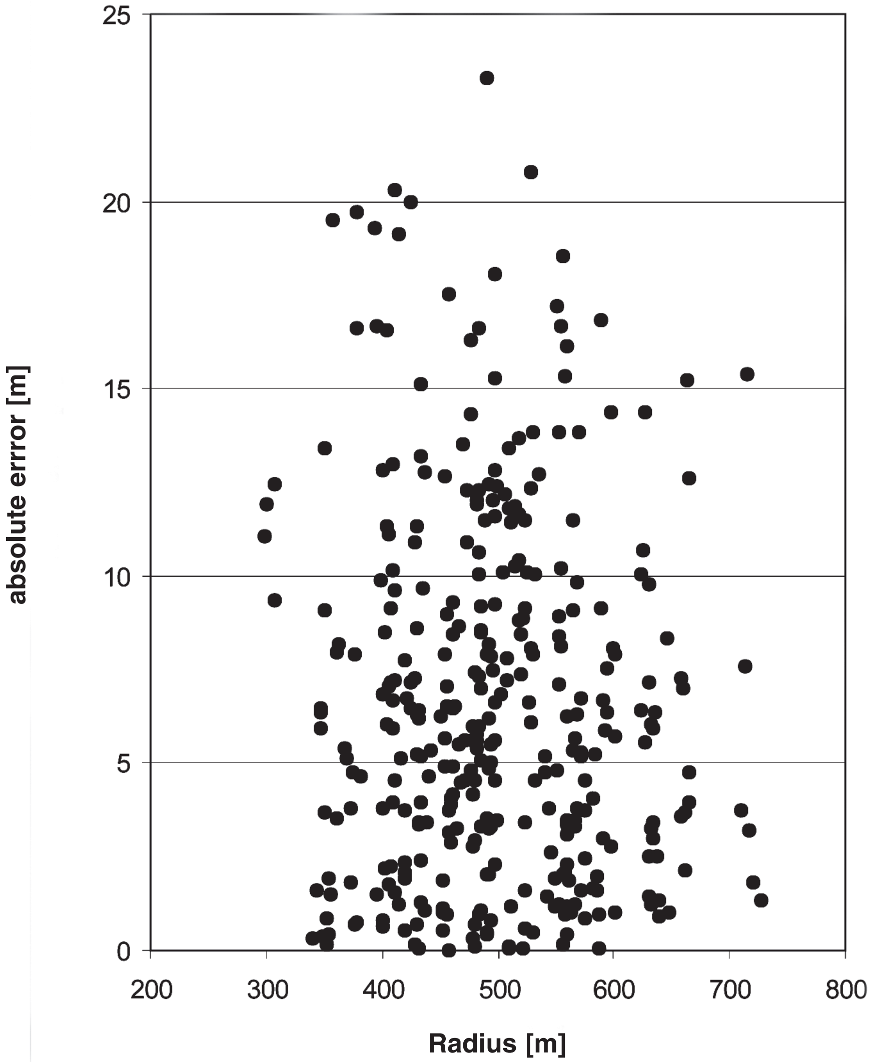

Fig. 8 - Values of the radius of the anticlines obtained by the inversion with an (3.2.2) ANN. The absolute error is shown as a function of the true depth.

the anticline and the depth of the bottom of the syncline respectively. These three parameters have been chosen because their determination by the classical interpretation technique is extremely difficult or totally inaccurate.

5. Conclusions

It has been demonstrated that qualitative gravity interpretation is possible with ANNs. The training and tests were done with features derived from the principal anomaly profiles. All fea-

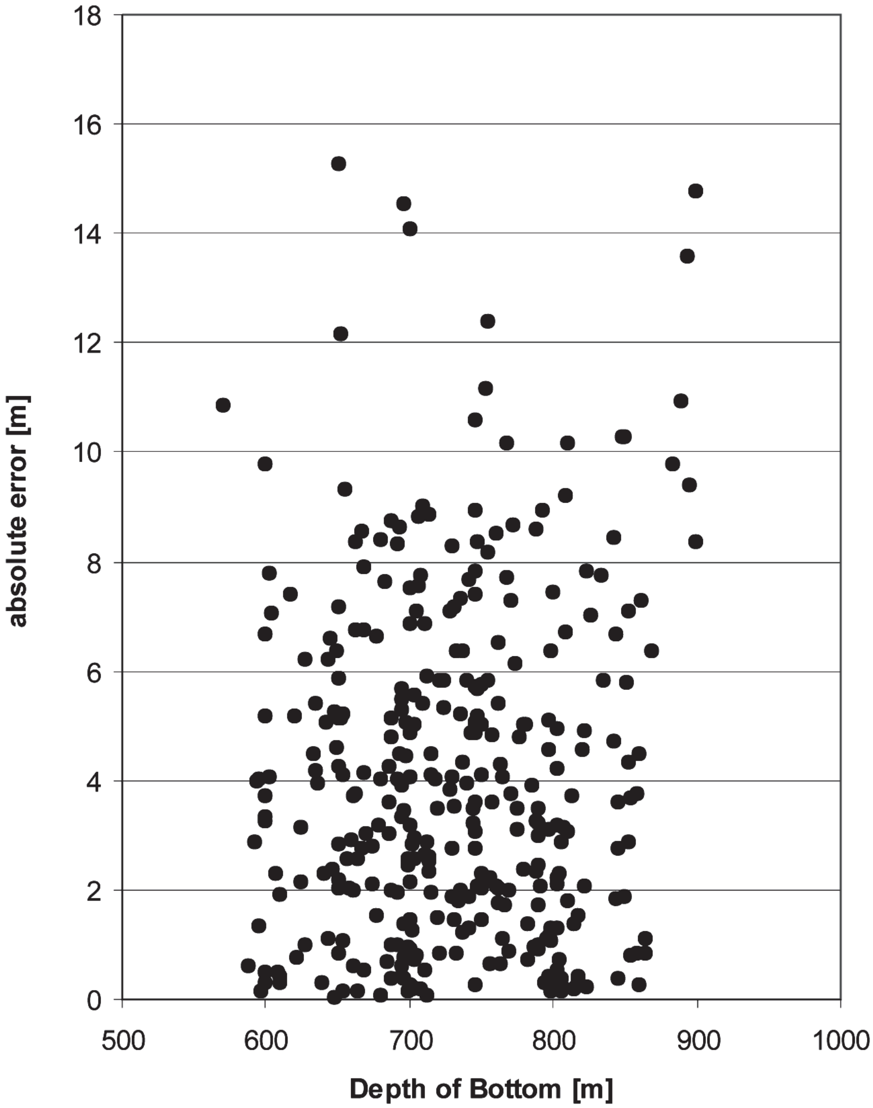

Fig. 9 - Values of the depth of the bottom of the synclines obtained by the inversion with an (3.2.2) ANN. The absolute error is shown as a function of the true depth.

tures were chosen in such a way that they did not depend on the density contrast and no estimation of it was needed. The results obtained for recognition are remarkably accurate and can be trusted at 99%.

The same kind of ANN was used for quantitative interpretation. After finding the right model the best values for the model's parameters were searched.

A training algorithm, which is less sensitive to local minimum and converges fast, was used (Levenberg-Marquardt Back-Propagation Approximation). It was found that the results are excellent when using very small networks. Networks with 2, 3 and 4 neurons respectively in the hidden layers are sufficient to solve the problems. These ANNs were tested with numerous anomalies. The ability of the networks to find the parameter values is remarkable. The average error, in percent of all bodies and all parameters lies at 2% and is never higher than 5%. When looking at the wide range of model parameters and the changes in density, which were used for testing the ANNs, this result is excellent.

Because all the calculations were based on synthetic data the capacity of ANN to interpret real data still has to be tested.

References

Freeman J. A. and Skapura D. M.; 1991: *Neural Networks*. Addison-Wesley Publishing Company, New York, 401 pp.

Grossberg S.; 1973: *Contour enhancement, short term memory, and consistencies in reverberating natural networks.* Studies in Applied Mathematics, **52**, 217-257.

Hagan M. T. and Menhaj M.; 1994: *Training Feed-forward Networks with the Marquardt algorithm: IEEE Transactions on Neural networks*, **5**, 6.

Hertz J., Krogh A. and Palmer R. G.; 1991: *Introduction to the theory of neural computation*. Addison-Wesley Publishing Company, New York, 327 pp.

Hecht-Nielsen R.; 1990: *Neurocomputing*. Addison-Wesley Publishing Company, New York, 433 pp.

McCulloch W. and Pitts W.; 1943: *A logical calculus of the ideas immanent in nervous activity*. Bulletin of Mathematical Biophysics, **5**, 115 - 133.

Rumelhart D. E. and Mc Lelland J. L.; 1989: *Parallel distributed processing*. Vol I. The MIT Press, Cambridge, 547 pp.

Simpson P. K.; 1990: *Artificial Neural Systems*. Pergamon Press, New York, 209 pp.

Wasserma P. D.; 1989: *Neural Computing*. Van Nostrand- Reinhold, New York, 348 pp.